JOURNAL OF OPTOELECTRONICS AND ADVANCED MATERIALS Vol. 10, No. 1, January 2008, p. 152 - 157

Osteoblast interaction with iron oxide nanoparticles coated with dextrin in cell culture

D. PREDOI*, R. A. VATASESCU-BALCAN[a]
National Institute of Materials Physics, P.O. Box. MG 07, 077125, Magurele, Romania
[a]Molecular Biology Center,University of Bucharest, 91-95 Splaiul Independenței, 76201, Bucharest 5, Romania

The iron oxide nanoparticles and iron oxide nanoparticles coated with dextrin have been synthesized using aqueous solution of ferric and ferrous ions and mixtures of dextrin with sodium salt. The size of the iron-oxide nanoparticles are controlled by the concentration of sodium salt in the medium. An average size of iron oxide and iron oxide coated with dextrin was found by transmission electron microscopie (TEM). The iron oxide nanoparticles are nearly spherical with an average diameter of about 8.0 ±1 nm. The iron oxide nanoparticles coated with dextrin appear to cluster-like aggregates. The average diameter of these nanoparticles is about 6±1 nm. The attachment of the dextrin on the particle surface was confirmed by FTIR spectroscopy and scanning electron microscopy (SEM). Osteoblasts used to determine the cell proliferation, viability and citotoxicity interaction with iron oxide nanoparticles coated with dextrin has been obtained from the upper part of the patient's femur.

(Received August 12, 2007; accepted January 10, 2008)

Keywords: Dextrin, Iron-oxide, Nanoparticles, Biocomposites

1. Introduction

Nanoscale magnetic structure offer great potential for Nanoscale magnetic structure offer great potential for advancements in electronics, optoelectronics, magnetic storage and biomedical applications. There is a great desire to prepare well-defined, discrete magnetic nanoparticles for both fundamental and social benefit. The excellent properties of these materials when compared with their bulk counterparts provide a very promising future for their use in this field [1-3]. Size and surface effects dominate the magnetic behavior of nanometric particles. The details of the relationships between shape, surface structure, composition and the resulting magnetic properties of magnetic nanoparticles are currently unclear.

Current research in the area of magnetic nanoparticles is focusing on applications were their unique properties will allow for significant advances in scientific technology. Magnetic nanoparticles show remarkable new phenomena such as superparamagnetism, high field irreversibility high saturation field. When placed in an external magnetic field their moments rapidly rotate into the direction of the magnetic field and enhance the magnetic flux. The benefit of such materials is that they could be designed with biocompatible surface stabilizers for new biomedical applications which included retinal detachment therapy [4-5], cell separation methods [6-7], tumor hyperthermia [8], improved MRI diagnostic contrast agents [9-12] and as magnetic field-guided carriers for localizing drug or radioactive therapies [13].

In this work, we report the synthesis of iron-oxide nanoparticles in aqueous solution in the presence of dextrin. Their characteristics were compared with iron-oxide nanoparticles. The samples were investigated by X-ray diffraction (XRD), transmission electron microscopy (TEM), scanning electron microscopy (SEM) and infrared spectroscopy. Osteoblasts used to determine the cell proliferation, viability and citotoxicity interaction with thin film and iron oxide nanoparticles coated with dextrin has been obtained from the upper part of the patient's femur.

2. Experimental

2.1. Materials

Ferrous chloride tetrahydrate ($FeCl_2 \cdot 4H_2O$), ferric chloride hexahidrate ($FeCl_3 \cdot 6H_2O$), natrium hydroxide (NaOH) and dextrin $(C_6H_{10}O_5)_n$ where purchased from Fluca (Merck), HCl these reagents were used directly as received. De-ionized water was used in the synthesis of nanoparticles, and in the rinsing of clusters.

2.2. Synthesis of iron-oxide nanoparticles

Iron-oxide nanoparticles were prepared according to the following procedure: ferrous chloride tetrahydrate ($FeCl_2 \cdot 4H_2O$) in 2M HCl and ferric chloride hexahydratate ($FeCl_3 \cdot 6H_2O$) were mixed at room temperature (Fe^{2+}/Fe^{3+} = ½). The mixture was dropped into 200 ml of 1.5M NaOH solution under vigorous stirring for about 30 min. The resulting precipitate was insolated in the magnetic field and the supernatant was removed from the precipitate by decantation. Purified deionised water was added to the precipitate and the solution decanted after centrifugation at 8000 rot/min. After repeating the lost procedure two times, 200 ml of 0.02M HCl solution was added to the precipitate

with continuous agitation. The product was separated by centrifugation (8000 rpm) and dried at 40 ^{o}C (sample 1).

2.3. Synthesis of iron-oxide-dextrin nanoparticles

Dextrin solution (20 g in 100 ml of water) was heated at 90 ^{o}C for 1h with continuous agitation (200 rot/min). Then 40 ml of 5M NaOH was added to the solution.

Ferrite solution (30 ml) containing stoichiometric ratio of 1:2 ferrous chloride tetrahydrate ($FeCl_2 \cdot 4H_2O$) and ferric chloride hexahydratate ($FeCl_3 \cdot 6H_2O$) was added dropwise to the solution. The suspension was incubated for 1h at 90 ^{o}C for 1h with gentle stirring. The 5M NaOH was added dropwise to obtain a pH of 11. The precipitate were centrifuged and washed with deionized water. The product was separated by centrifugation (10000 rpm) and dried at 40 ^{o}C (sample 2).

2.4. Sample characterization

Crystallographic analysis of the samples was performed by powder X-ray diffraction (XRD). Diffraction patterns of intensity vs. 2θ were recorded with a Philips PW 1050 diffractometer. A continuous scan mode was used to collect 2θ data from 10 to 70^0.

A transmission electron microscopy (TEM) was carried out on a JEOL 200 CX. The specimen for TEM imaging was prepared from the particles suspension in deionized water. A drop of well-dispersed supernatant was placed on a carbon – coated 200 mesh copper grid, followed by drying the sample at ambient conditions before it is attached to the sample holder on the microscope.

IR spectroscopic studies were performed in the range 1800-400 cm^{-1} using a FTIR Spectrum BX spectrometer. Samples dehydrated at room temperature were pelleted with dried KBr. On the powders, Differential thermogravimetric analysis (TGA, DTG) and differential thermal analysis (DTA) of these samples were carried out on a Perkin Elmer Diamond thermal analyzer in the presence of static air at a linear heating rate of 10^0 from 25 ^{o}C to 800 ^{o}C.

2.5. Cell culture

Osteoblasts were grown in Dulbecco Modified Eagle's Medium (DMEM) supplied with 10% fetal bovine serum, DMEM sodium pyruvate, 2% glutamine and antibiotic mix. Medium compounds were purchased from Gibco (UK). The cells were incubated at 37 °C, 5% CO_2 and the split was performed using tripsin-EDTA solution 1x (Sigma-Aldrich) and phosphate-buffered saline (PBS) from Gibco.

Osteoblasts used to determine the cell proliferation, viability and citotoxicity interaction with thin film and iron oxide coated with dextrin has been obtained from the upper part of the patient's femur. These patients undergo the surgery intervention in arthritis disease when the haunch articulation is removing.

Primary osteoblast culture from bone explants was designed according to Gallagher et al (1996) protocol [14-16]. The pieces from bone tissue are transferred into a sterile recipient with PBS. Obtained tissue is detached from soft conjunctive tissue of the external bone area. The tissue is rinsed in sterile PBS and removed in Petri dishes which contain a small volume of sterile PBS proportionally to the size of the pieces.

Next step was to place the explant fragments in DMEM with antibiotics supply, washing successively with antibody solutions, cultivate in DMEM medium supplied with 15% Bovine Serum Albumin (BSA), 2% glutamine and buffered with natrium bicarbonate.

The first osteoblasts from explants arises after 7-10 days of incubation (5% CO_2 atmosphere, T=37 ^{o}C) and were suitable for split after 4-6 weeks; after the second passage, the culture contains strictly osteoblast cells. Subsequent splits were performed at confluence (2×10^6 cells/plate) in about 10 days, with a 1:3 ratio. Confluent cultures have been treated with trypsin for 2-3 min and then centrifuged at 1.500 rpm for 10 min. Cells were re-suspended in minimal DMEM volume, counted with Burker-Turk chamber and evenly distributed on sterile supports, previously treated with polylisine.

2.6. Cell viability

Biocompatibility test of the thin film and iron oxide coated with dextrin has been done using primary osteoblast cell line. After osteoblast culture achievement, the cells were treated with trypsin 0.05% and spited in 35/35 mm Petri dish.

Cells were seeded at a density of 10^5 cells/ml in Petri dish and incubated on thin film for 48 hours. In contrast, osteoblast cells were seeded at a the same density of 10^5 cells/ml in Petri dish and incubated with sample 2 at 1% concentration for 2, 4, 12 and 24 hours. The cell viability was determined by MTT (3-(4, 5-dimethylthiazol-2-yl)-2,5-diphenyltetrazolium bromide) reduction test. The cells were incubated (5% CO_2 atmosphere, T=37 ^{o}C) for 4h with MTT (0.1 mg/ml).

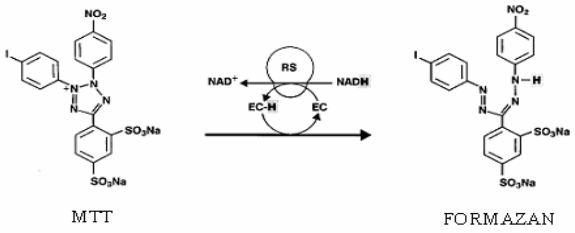

Fig. 1. MTT is reduced to formazan in mitochondria of the cells.

The viability cell number is directly proportional to the production of formazan. The isopropanol was added to dissolve the insoluble purple formazan product into a

colored solution. The absorbance was quantified by measuring the wavelength at 595 nm by TECAN spectrophotometer.

3. Results and discussions

The iron oxide nanoparticles coated with dextrin were previously characterized by X-ray diffraction (XRD) [17].

Fig. 2 shows TEM images and grain size distributions from TEM of sample1.

As can be seen in Fig. 2 the iron oxide nanoparticles are nearly spherical with an average diameter of about 8.0 ±1 nm. The iron oxide nanoparticles coated with dextrin (Fig. 3) appear to cluster-like aggregates. The average diameter of these nanoparticles is about 6.0 ±1 nm.

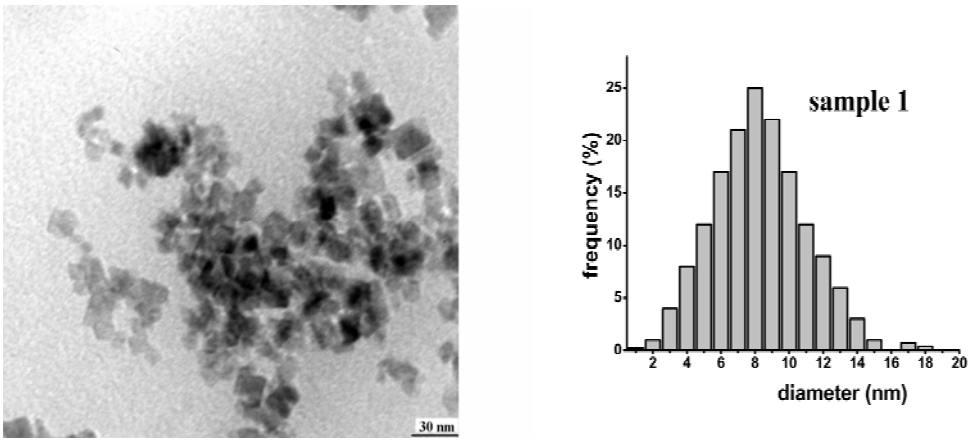

Fig. 2. Transmission electron microscopy images of iron oxide nanoparticles (1) and grain size distribution from TEM of iron oxide (2).

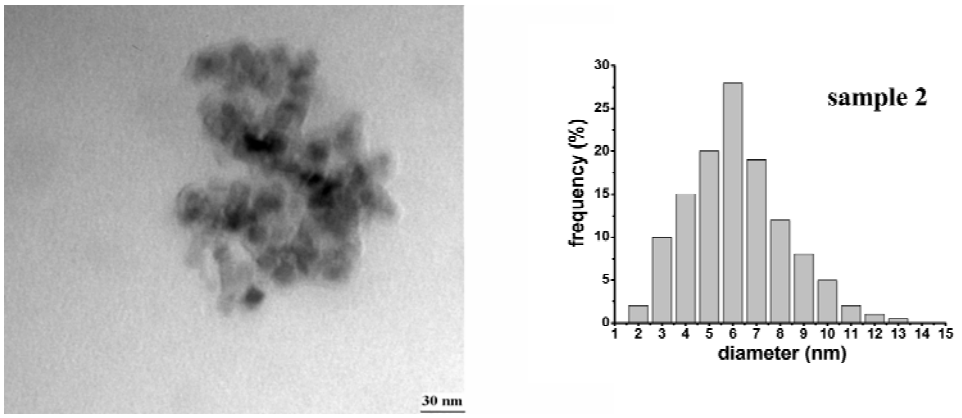

Fig. 3. TEM images of iron oxide nanoparticles coated dextrin (1) and grain size distribution from TEM of iron oxide nanoparticles coated with dextrin (2).

Results obtained by scanning electron microscopy analysis for the iron oxide nanoparticles coated dextrin powder and for thin films of iron oxide coated with dextrin are shown in Fig. 4.

To analyze the morphology and crystallite size, SEM analysis has been conducted. As confirmed by SEM micrograph the attachment of the dextrin on the iron oxide nanoparticles surface. The iron oxide nanoparticles seemed to be mostly incorporated in the dextrin spheres and no free magnetic particles were discernable in SEM.

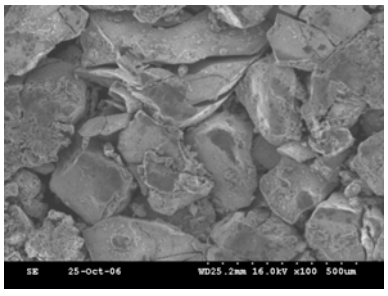

Fig. 4. Typical SEM image of iron oxide nanoparticles coated dextrin.

The attachment of the dextrin on the particle surface was confirmed by FTIR spectroscopy. Fig. 5 gives the IR transmission spectra of iron oxide, iron oxide nanoparticles coated with dextrin and pure dextrin. Correspondingly, the assignments of the absorption band in the spectra were listed in Table 1.

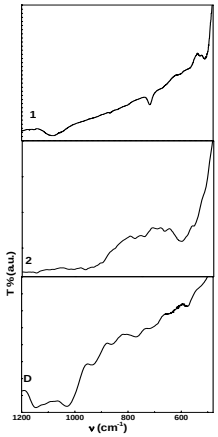

Fig. 5. The FT-IR spectra of samples: (1) iron oxide; (2) iron oxide nanoparticles coated with dextrin and pure dextrin (D).

The spectrum of the latter colloidal iron oxide contains characteristic OH stretching (ν OH) and HOH bending (δ OH) vibrational bands at 3400 cm^{-1} and 1600 cm^{-1} due to the adsorbed water in the sample [18]. The band observed at 620 cm^{-1} -580 cm^{-1} corresponds to the stretching vibration M_{Th}- O-M_{Oh}, and M_{Th}- M_{Oh} ($\nu_3 \approx$ 350-400 cm^{-1}), where M_{Th} and M_{Oh} correspond to the metal occupying tetrahedral and octahedral positions respectively [19-20]. The stretching vibration ν(Fe-O) correspond of tetrahedral iron atoms.

A typical IR spectrum of the dextrin presents bands at 3365 cm^{-1} (O-H), 2851-2940 cm^{-1} (C-H), 1040-1110 cm^{-1} (C-O) [21].

The spectra of the iron oxide nanoparticles coated with dextrin just had little difference with the ones of pure dextrin, witch indicated that the interactions between dextrin and iron oxide nanoparticles were intermolecular interactions.

Table 1. Assignment of the absorption bands in the IR spectra.

Dextrin	Iron oxide nanoparticles coated with dextrin (cm^{-1})	Iron-oxide nanoparticles (cm^{-1})	Assignments
3500-3200	3500	3500	ν^* H- O……H
2925	2917		ν^*_{as} C-H of $-CH_2$
1455; 1370	1460; 1350	1600	δ^*H-C-OH
1277	1273		δ^*H-C-OH
1152	1160		ν^*_s C-O-C
800-1200	800-1200		C-C
	590	590	Fe-O

Notations used:
ν^*: stretching vibration; ν^*_{as}: asymmetrical stretching vibration; ν^*_s: symmetrical stretching vibration; δ^*: deformation

MTT assay is a laboratory test and a standard colorimetric assay (an assay which measures changes in colour) for measuring cellular proliferation (cell growth). It is used to determine cytotoxicity of potential medicinal agents and other toxic materials.

Yellow MTT (3-(4,5-Dimethylthiazol-2-yl)-2,5-diphenyltetrazolium bromide, a tetrazole) is reduced to purple formazan in the mitochondria of living cells. A solubilization solution (isopropanol) is added to dissolve the insoluble purple formazan product into a colored solution. The absorbance of this colored solution can be quantified by measuring at a certain wavelength (usually between 500 and 600 nm) by a spectrophotometer.

This reduction takes place only when mitochondrial reductase enzymes are active, and therefore conversion is directly related to the number of viable cells. When the amount of purple formazan produced by cells treated with an agent is compared with the amount of formazan produced by untreated control cells, the effectiveness of the agent in causing death of cells can be deduced, through the production of a dose-response curve.

Osteoblast cells were permanent monitored to detect any possible influence due to iron oxide coated with dextrin (sample 2) that might modify the cell growth, viability and proliferation. This study represents one of the key-step in cell biology, mitochondrial dehydrogenases being essential.

The results obtained after MTT assay have revealed (Table 2) as we expected, the fact that control sample has one of the greatest value (0.3363). This value is also established by the high intensity of the color (deep purple) in control due to the amount of formazan produced by cells.

Table 2. Absorbance values at 595 nm.

Samples	DO_{595nm}	Viability (%)
Control	0.336333	100
sample 2 – 2 hours	0.16845	50.08424
sample 2 – 4 hours	0.201667	59.96034
sample 2 – 12 hours	0.3037	90.29732

The study reveals that osteoblast cells' growing with sample 2 for 24 hours present the highest peak, while those incubated for only 2 hours has the smallest peak (Fig. 6). The absorbance value (0,3363) of control is higher comparing to the cells incubated with iron oxide coated with dextrin for 2, 4 and 12 hours, but lower relating to cell's growing with the same bioceramic for 24 hours (Table 2).

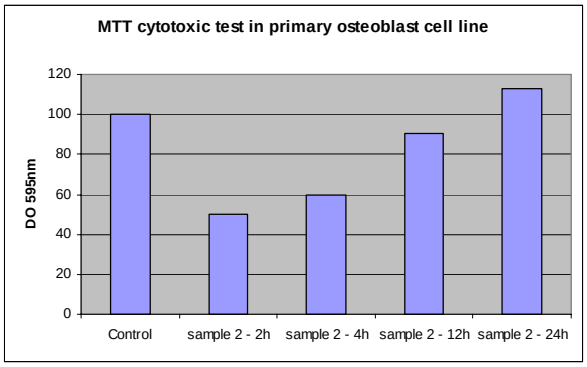

Fig. 6. MTT assay in osteoblast cell's growing with D15S bioceramic.

Cells' incubation with iron oxide coated with dextrin for 24 hours shown the increase of proliferation and viability (112,68%), comparing to the control (100%). In contrast, the osteoblast cells incubated with the same bioceramic for 2, 4 and 12 hours presented a growth inhibition and the decrease of viability, relating to control. Interestingly, after 2 hours of exposure with D15S and diminish in proliferation of the osteoblast cells, we observed a tendency of linear increase of viability and proliferation which is proportionally to the exposure interval (Fig. 6). This effect might be due to cells adaptation at interaction with bioceramics.

5. Conclusions

Iron oxide nanoparticles coated with the dextrin were synthesized by coprecipitation of two mains solutions $FeCl_2 \cdot 4H_2O$ and $FeCl_3 \cdot 6H_2O$ in a stoichiometric ratio 1:2 in dextrin solution adding 5M NaOH. The iron oxide phase was described to be a ferrite with properties of magnetite. The TEM images suggest that the use of dextrin in the material synthesis limits particle size. The iron oxide- dextrin preparation generates particles that are significantly smaller than the iron oxide preparation in which dextrin is not present. Moreover the adsorption dextrin iron oxide nanoparticles were evidenced by FTIR spectroscopy and were confirmed by TG analysis.

In the same manner as previously, cells' incubation in the presence of iron oxide coated with dextrin can modify parameters of cell growing causing the increase or decrease of proliferation and viability relating to control. Thus, the exposure period (2, 4, 12 or 24 hours) could be an important factor in osteoblast cell's growing.

Acknowledgements

The authors are greatly indebted to Prof. Dr. Marieta Costache for useful discussions. This work was financially supported by Science and Technology Ministry of Romania (Project CEEX_24/2005 and the Project CEEX_150/2006 VIASAN Program). We gratefully acknowledge l'Institut de Chimie de la Matière Condensée de Bordeaux for the permission to use their laboratories in the sample characterizations.

References

[1] R. M. Cornell, U. Schwertmann, The Iron Oxides; Wiley-VCH: Weinheim, Germany, (2003).
[2] J. M. Perez, F. J. Simeone, Y. Saechi, L. Josephson, R. J. Weissleder, Am. Chem. Soc. **125**, 10192 (2003).
[3] A.I. Anton, J. Magn. Magn. Mater. **85**, 137 (1990).
[4] P. Oswald, O. Clement, C. Chambon, E. Claeys, E. Fuja, G. Magn. Reson. Imaging **15**, 1025 (1997).
[5] L. Fu, V. P. Dravid, D. L. Jhonson, Appl. Surf. Sci. **181**, 173 (2001).
[6] D. L. Leslie-Pelecky, Chem. Mater. **8**, 1770 (1996).
[7] E. M. Moreno, M. Zayat, M. P. Morales, C. J. Serna, A. Roig, D. Levy, Langmuir **18**, 4972 (2002).
[8] J. Lee, T. Isobe, M. Senna, J. Colloid. Interface Sci. **177**, 490 (1996).
[9] B. D. Cullity, In elements of X-ray Diffractions, Additiond Wesley: Reading, MA, 1978.
[10] M. L. Hair, J. Non-Cryst. Solids **19**, 299 (1975).
[11] E. Barrodo, F. Prieto, J. Medina, F. A. Lopez, J. Alloys. Compd. **335**, 203 (2002).
[12] J. L. Martin de Vidales, A. Lopez-Delgado, E. Vila, F. A. Lopez, J. Alloys. Compd. **287**, 276 (1999).
[13] H. R. Wang, K. M. Chen, Colloids and Surfaces A : Physicochem. Eng. Aspects **281**, 190 (2006).
[14] A. J. Gallagher, R. Gundle, N. J. Beresford, Isolation and culture of bone forming cells (osteoblasts) from human bone, Human Cell Culture Protocols (Jones, E.G., eds.) 233-263, 1996.
[15] A. M. Parfitt, Osteonal and hemi-osteonal remodeling: the spatial and temporal framework for signal traffic in adult human bone, J. Cell. Biochem. **55**, 273-276 (1994).

[16] P. G. Robey, A. L. Boskey, The biochemistry of bone in osteoporosis (Marcus, R., Feldman, D., Bilezikian, J. P., Kelsey, J., eds), Academic Press, New York, 95-183, 1995.
[17] D. Predoi, Digest Journal of Nanomaterials and Biostructures **2**(1), 169 (2007).
[18] M. L. Hair, J. Non-Cryst. Solids **19**, 299 (1975).
[19] E. Barrodo, F. Prieto, J. Medina, F. A. Lopez, J. Alloys. Compd. **335**, 203 (2002).
[20] J. L. Martin de Vidales, A. Lopez-Delgado, E. Vila, F. A. Lopez, J. Alloys. Compd. **287**, 276 (1999).
[21] H. R. Wang, K. M. Chen, Colloids and Surfaces A: Physicochem. Eng. Aspects **281**, 190 (2006).

*Corresponding author: dpredoi_68@yahoo.com